The influence of charge on the multiple thermal transitions observed in xanthan

A. H. Abbaszadeh[1], M. Lad[1a], G. A. Morris[1b,✉], W. MacNaughtan[1], G. Sworn[2] and T. J. Foster[1]

[1] *Division of Food Sciences, School of Biosciences, University of Nottingham, Sutton Bonington Campus, Loughborough, LE12 5RD, UK. Member of the European Polysaccharide Network of Excellence (EPNOE).*

[2] *DuPont, Danisco France SAS, 20 rue Brunel, 75017 Paris, France.*

[a] *Current address: Fonterra Research and Development Centre, Fonterra Co-operative Group Ltd, Palmerston North, New Zealand.*

[b] *Current address: Department of Chemical Sciences, School of Applied Sciences, University of Huddersfield, Queensgate, Huddersfield, HD1 3DH, UK.*

✉Corresponding author:

Tel: +44 (0) 1484 473871

Fax: +44 (0) 1484 472182

Email: g.morris@hud.ac.uk

Highlights

- Transitions in xanthan with charged pyruvate groups occur at lower temperatures
- A mass action model describes changes in transition temperature with salt addition
- Xanthans having biphasic transitions have phases with different levels of pyruvate
- Salt differentially affects transition temperatures of different pyruvate phases
- A linear relation exists between ln[NaCl] and the reciprocal transition temperature

Abstract

Helix-coil transitions in xanthans occur at lower temperatures when the pyruvate group is charged, destabilising the polymer chains. Increasing salt content increases the transition temperature by reducing the effective charge on the pyruvate. A simple equivalent mass action model predicts how transition temperatures change as a function of salt concentration. The functional form of the change in transition temperature (1/T) versus natural log (salt concentration) is approximately linear and similar to more traditional polyelectrolyte theories. Transition temperatures in xanthans containing nominally homogeneous pyruvate contents show biphasic transitions, this is because the phases contain different pyruvate levels, however the transitions approach one another in temperature and eventually merge as salt content is increased. It is proposed that pyruvate groups, despite being present at a lower concentration relative to glucuronic acid, dominate the charge interactions due to their location on the outside of the helices. (143 words)

Keywords: xanthan, pyruvate, charge screening, salt content, transition temperatures, Differential Scanning Calorimetry (DSC).

1. Introduction

Polysaccharides are used as additives to improve the stabilisation of food products by increasing viscosity or creating a gel. Xanthan is a commonly used and thoroughly investigated polymer and is known to have charged groups. These charged groups profoundly influence the functioning of the polymer; for instance, the presence of a high charge density is thought to destabilise the interactions between individual chains of the polymer (Morris, Rees, Young, Walkinshaw, & Darke, 1977; Shatwell, Sutherland, Dea, & Ross-Murphy, 1990). It is of interest to examine these properties in more detail. Moreover, the extent to which these interactions are influenced by the presence of other biopolymers is still an area which receives extensive investigation.

Polysaccharides are commonly observed to possess a high tendency to associate (Burchard, 2001). This association is usually caused by the abundant hydroxyl or amino groups present in the macromolecules and which easily undergo hydrogen bonding. For polysaccharides forming three-dimensional networks under specific conditions *i.e*. gel formation, these interactions comprise hydrogen, dipole and ionic bonding, solvent partition effects and structural interactions at tie points. Individually, these interactions are so weak that conformational stability is achieved only when a large number of them occur simultaneously or cooperatively. The presence of charged groups on polysaccharide chains might be expected to oppose this natural tendency to associate and so affect the propensity to form viscous solutions and gels as well as interactions (Khouryieh, Herald, Aramouni, & Alavi 2007). Biopolymer mixtures may also undergo isothermal phase transitions due to changes in external conditions, such as ionic strength, pH and temperature. Recently Morris (2019) has sought to explain the ordered conformation of xanthan in solution, concluding that, as for other protein and polysaccharide systems, interchangeability of structures between single and double helices should not be unexpected, as a result of their environmental conditions. Indeed, for xanthans with varying acetate content (known for their helix stabilisation effects) Morrison et al. (2004) conclude that low acetate xanthans exist in a flexible single stranded form, as opposed to a more rigid double helix.

A number of combinations of xanthan with other polysaccharides demonstrating synergistic interactions have been identified. The most familiar systems that show synergistic interaction are mixtures of xanthan and galactomannan or glucomannan (Morris, 1990; Williams & Philips, 1995; Morris & Wilde, 1997; Abbaszadeh, MacNaughtan, Sworn, & Foster, 2016) where interactions between the backbones of the molecules have been proposed. However, in the present work we are concerned with the main helix-coil transition as well as residual helix-coil transitions in xanthan after any other such interactions have taken place, consequently one xanthan/ glucomannan mixture has been studied in this work from the limited perspective of examining whether the presence of the other polysaccharide changes the temperature or other characteristics of the remaining thermal or “charge” transitions. This work arose from the observation that the temperature of multiple transitions in some samples of xanthan were observed to increase and move together as the salt (ionic sodium) content was increased. We proposed in an earlier paper that these multiple transitions were due to phases in the xanthan having different concentrations of pyruvate and hence different charges as indeed has been reported earlier (Kitamura, Takeo, Kuge, & Stokke, 1991; Agoub, Smith, Giannouli Richardson & Morris, 2007). We have found subsequently that a very simple consideration of a dissociation/association constant of the positively charged sodium with negatively charged pyruvate appears to explain a large part of this behaviour. Whilst realising that this must only be a crude approximation we describe the method and the results in the hope that this might be of use to other research relating to and understanding the behaviour of charged polymers.

1.1 The effect of charge on xanthan

Xanthan is a charged polymer whose properties are profoundly determined by pH and ionic concentration (Pastor, Costell, Izquierdo, & Durán, 1994; Morris, Puaud, Li, Lui, Mitchell, & Harding, 2001; Morris & Harding, 2009). The effect of charge screening on the xanthan can be thought of very simply as an ionic atmosphere of positively charged ions surrounding the negative charges on the glucuronic acid and pyruvate groups of the xanthan (**Figure 1**).

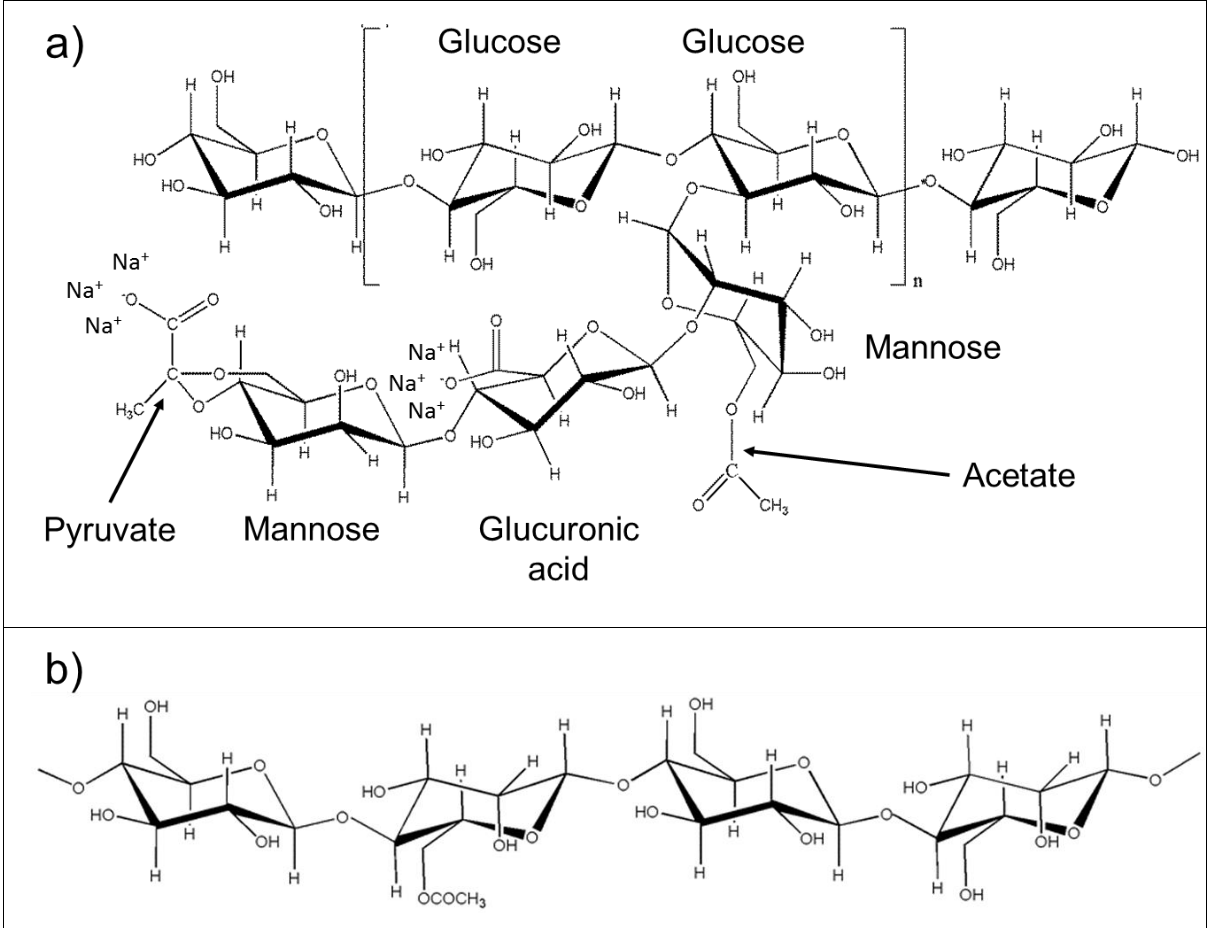

Figure 1 a) An *idealised view of the xanthan molecule with the pyruvate and glucuronic acid sites highlighted and the presence of sodium ions indicated. This view does not show possible variations in distribution of pyruvate content along the main chain or any steric details of structure. b) Konjac Glucomannan (KGM) is an example of a polysaccharide that interacts with xanthan via backbone rather than charge interactions.*

It is proposed that the transition temperature will be a function of the overall charge on the molecule; the higher the charge on the xanthan, the more destabilisation or repulsion between chains will occur and therefore the lower the transition temperature. Therefore, we would expect that increasing the overall salt concentration will result in a higher transition temperature (Shatwell, *et al.*, 1990) although the exact form that this would take is unknown. This would also suggest that there should be a limiting transition temperature for an uncharged or minimally charged polymer, as well as for a fully charged system.

We examine the effect of salt on the thermal transitions measured in xanthans using DSC and also whether the presence of other polysaccharides including other xanthans has a significant effect on these transitions. Our hypothesis is that the helix-coil transition is solely dependent on the charge present on the xanthan and we examine the consequences of this proposal.

2. Materials and methods

2.1 Sample preparation

A range of xanthan samples having variable pyruvate and approximately constant acetate contents (5 - 6 %) was supplied by Danisco. These comprised Standard Pyruvate Xanthan (SPX nominally 3.8%), Low Pyruvate Xanthan (LPX nominally 2.2 %) and High Pyruvate Xanthan (HPX nominally 6.5%). Working on a maximum pyruvate content, where every site is substituted, of about 9.5%, and depending on the exact method of calculation, the stoichiometric ratios for our 2 proposed phases in standard xanthan of 3 and 5% are 1 in 3 and slightly less than 2 in 3 substituted sites respectively. All xanthans were initially dialysed against distilled water. Glucomannan (Propol RS; High Mwt. (KGM)) was bought from the Shimizu Chemical Corporation. Sodium azide and sodium chloride were bought from Acros and Fisher respectively. Single xanthans, mixtures of xanthans at different pyruvate contents and mixtures of glucomannan with xanthans, were formed by initially dispersing the polymers in pre-prepared aqueous salt solutions at room temperature, shearing using a magnetic flea followed by heating at ~90 ºC for 20 min. Salt solutions at salt levels of 10 mM (0.059 % sodium chloride) and 40 mM NaCl (0.234 % sodium chloride) were prepared using reverse osmosis water. Sample polymer concentrations of 1% or 0.5/0.5% for mixed systems w/w in aqueous salt solutions were used. The viscous solutions were then cooled to room temperature and left overnight before Differential Scanning Calorimetry (DSC) was performed.

2.2 High sensitivity Differential Scanning Calorimetry (μDSC)

Microcalorimetry was carried out using a Micro DSC III (Setaram, Caluire, France) with cells made from Hastalloy. Approximately 800 mg of material were weighed into a cell and sealed with a Hastalloy screw top and O ring. Temperature was increased at 1°C min^{-1}. Micro-DSC is distinguished from "conventional" DSC by the increased sensitivity of the instrument, larger sample volumes and lower scan rates. Conventional DSC can only just detect the small heat flows associated with these transitions; typically, hydrocolloid solutions where the concentration is of the order 1% or less, and then only if conditions such as baseline curvature and slope are optimal. The helix-coil transition of xanthan has been followed extensively using micro-DSC (Annable, Fitton, Harris, Phillips, & Williams, 1994; Goycoolea, Morris, &

Gidley, 1995; Bresolin, Milas, Rinaudo, Reicher, & Ganter, 1999). In this work micro-DSC has been used to investigate the helix-coil transition temperature of the supplied xanthans at 2 different salt levels:10 mM (0.059 % sodium chloride) and 40 mM NaCl (0.234 % sodium chloride).

Sample solutions or gels were carefully placed in the cell and firstly cooled to a starting temperature of 10°C. Samples were run at rates of 1°Cmin^{-1} from 10 to 110°C, cooled and reheats performed. The reference cell was filled with water, the weight of which was calculated to match the overall heat capacity of the sample. In practice, with such small concentrations of hydrocolloid, the cell contents could simply be matched for weight. Temperature values were determined using Setaram software with a linear interpolated baseline, based on an extension of the trace before and after the thermal event. Heat and temperature calibrations were preset by the manufacturer and checked using the transition in naphthalene.

2.3 Manufacture of xanthans

The method used by the manufacturer to produce xanthans of different pyruvate contents was as follows. The SPX and HPX samples were a result of natural variations in the concentration of the functional groups produced during the fermentation process by *Xanthomonas campestris*. Medium and high pyruvate batches were then selected from the available range of concentrations. The low pyruvate content of the LPX sample was produced by subjecting the fermentation broth to heat treatment in acidic conditions.

2.4 Measurement of functional group content

The acetate and pyruvate levels (%w/w) were supplied by the manufacturer (see **Table 1** for pyruvate levels). The final percentage quoted can depend on the method of calculation, consequently the values here are higher than values quoted in other work (Kool, Schols, Delahaije, Sworn, Wierenga, & Gruppen, 2013).

2.5 The effect of charge and model properties

The effect of charge screening on xanthan can be described by a simple model involving an ionic atmosphere of positively charged ions shielding the negative charges on the xanthan. This can be approximated by an effective equilibrium constant describing the interaction as though it were a single positive charge interacting with and neutralising a single negative charge. We call this an equivalent mass action model. In addition, there is a “sensitivity” parameter Δ which describes the dependence of the transition temperature on the degree of charge and hence destabilisation of the polymer. This is subtracted from the limiting transition Tm corresponding to the situation of no charge on the polymer. Δ has a negative sign and units of °C Litres/Mole. The transition temperature is assumed to be a simple linear function of charge and the sensitivity parameter effectively incorporates the various constants required for the fit. There is also an upper limiting transition temperature T_m for the transition temperature of an uncharged system, which was initially set to the highest value observed for any sample (approximately 90-100°C) however this will be discussed in more detail in the discussion. Interestingly there should also be lower limiting values corresponding to fully charged systems. This was not pursued here. The details of the model and the fitting procedure are shown in **Figure 2**.

Simple Equivalent Mass Action Model

Whilst an effective 1-1 interaction is considered here, it is recognized that the ions will be in the form of an ion atmosphere

1) $Na^+ + P^- \longleftrightarrow NaP$

2) Equilibrium constant = K = [NaP]/[Na^+][P^-]

3) Concentrations of {Charged Pyruvate + uncharged Pyruvate = Total Pyruvate}:
   $[P^-] + [NaP] = [P]_t$

4) Transition temperature (T_t) decreases as charge on pyruvate increases

5) Transition temperature proportional to charged pyruvate concentration: $T_t = Tm + \Delta X[P^-]$:
   where Δ = sensitivity parameter; negative value

6) Limiting transition temperature T_m for uncharged species. Fix value

7) Optimise by fitting experimental data to (T_t) by changing K and Δ

8) $[P]_t$ supplied by manufacturer: [Na+] assumed to be constant under most conditions and equal to bulk concentration (see text for further consideration of this point)

Figure 2 *The model and optimisation procedure.* T_m *can be estimated independently thus lowering the overall number of fitting parameters, particularly if independent parameters for 2 phases are considered. The limitations of this are discussed in the text. For the biphasic transitions a range of fitting parameters can be used from 1 equilibrium constant and sensitivity parameter for both phases through to 2 of each.*

A simple picture of the model is that for a highly charged phase *i.e.* a polymer phase containing a high pyruvate content, it will require a greater amount of sodium ions (higher concentration) to neutralise the negative charge on the polymer. Therefore, the 2 transitions will behave differently. The low pyruvate phase will reach equilibrium *i.e.* an effectively uncharged state, at lower sodium concentrations and in a way determined by the equilibrium constant and equivalent mass action model. Therefore, the dependence on sodium concentration will be different as shown in **Figures 4** and **6**.

The equilibrium constant describes the ratio of uncharged to charged species. Two separate phases have been observed in the case of standard xanthan (SPX) as shown on **Figure 3**. The determination of the properties of these phases is discussed further in Abbazadeh et al. (2015).

All temperatures relate to the peak temperature as measured by micro-DSC. In the fitting regime the two parameters; sensitivity and equilibrium constant Δ and K, could be "traded" against each other; hence setting T_m has the advantage of rendering the fitting procedure more robust with fewer fitting parameters. In practice the limiting temperature T_m when optimised, fell in the range 90 – 95°C. The model equations were embedded in Microsoft Excel and the Solver routine was used for all fitting and optimisation.

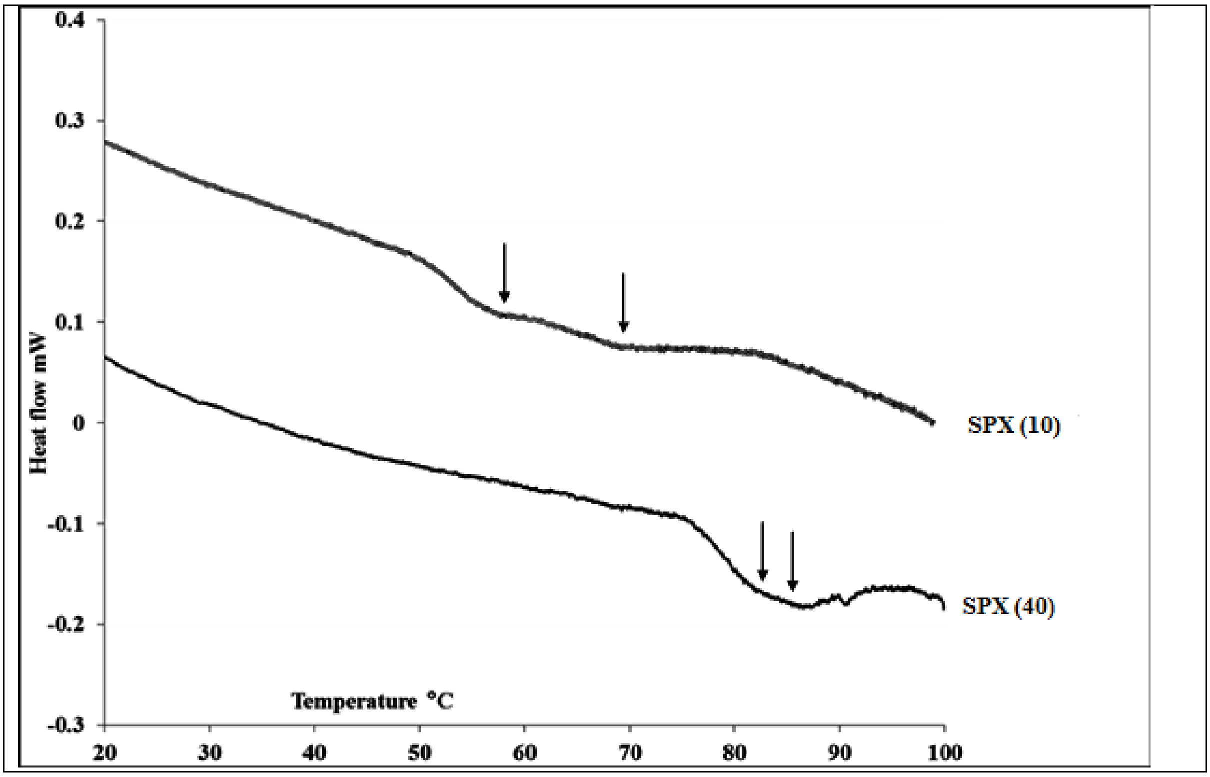

Figure 3 *The original DSC data showing the biphasic trace for standard pyruvate xanthan in 10 mM NaCl going to an apparent monophasic transition at 40 mM NaCl. The single transition is actually still 2 distinct transitions close in temperature. Xanthan concentration was 1%.*

3. Results and discussion

Using the optimisation routine, a fit using one equilibrium constant and two sensitivity parameters (K + Δ_1 and Δ_2), for each of the phases, was used (see **Table 1**). This was justified on the assumption that the interaction of sodium with each of the phases of different charge would probably be the same however the sensitivity of the phase transition would be more likely to be dependent on the charge. This fit enabled the solid line plots in **Figures 4** and **6** for the two transitions observed in SPX (**Figure 3**) to be plotted as a function of sodium chloride concentration. T_m, the limiting transition, was actually optimised on **Figure 4** but could be set to any other value and values above 100°C have been observed in previous work (Christensen & Smidsrød, 1991). Fits were optimised by minimising the sum of the squares of the difference between the experimentally measured transition temperatures and the temperatures predicted by the model by changing the aforementioned parameters. The fits are good (the sum of the square differences are low) and satisfyingly describe the essential observation here, namely that the 2 transitions observed in the SPX sample increase and move together in temperature as the salt content is increased. The value for the equilibrium constant of the proposed reaction of the sodium ion with pyruvate is low, of the order of 100 or so. These parameters can be varied substantially and still provide an apparently good fit by eye. The equivalent equilibrium constant derived from literature values for the Ka of pyruvic acid ranges between approximately 300 and 900.

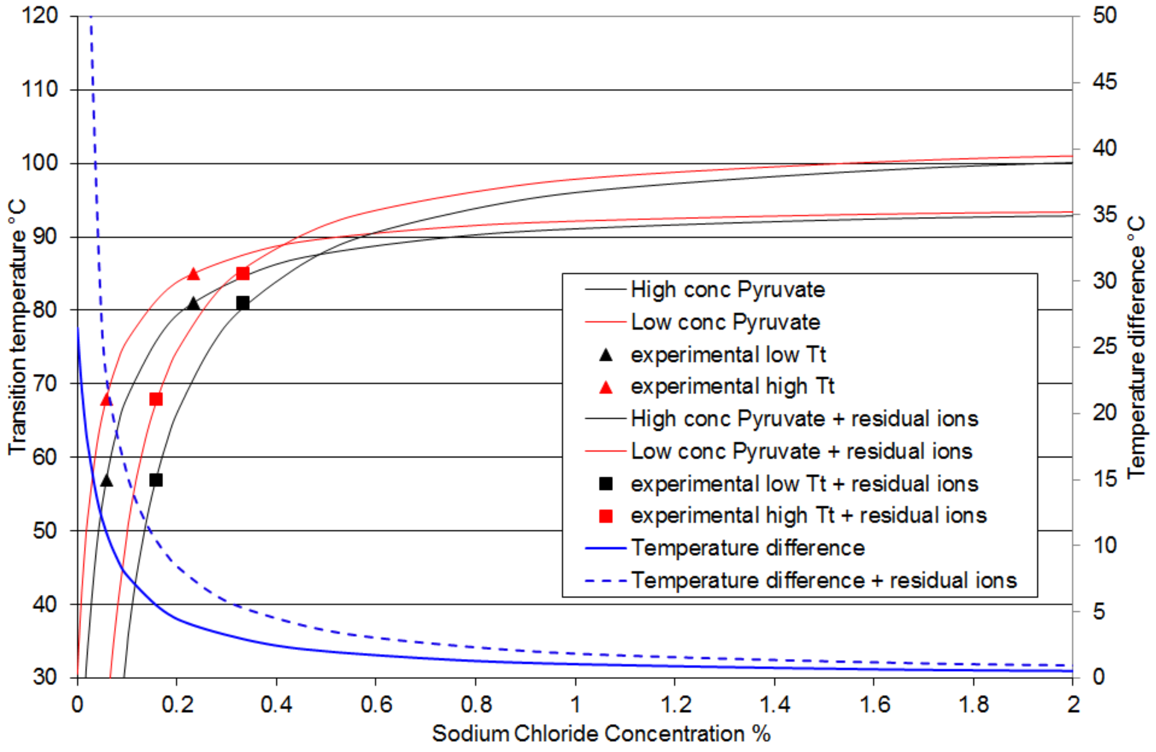

***Figure 4** shows the predicted transition temperatures for the 2 phases shown on figure 3 as a function of salt concentration. Parameters for the model are T_m = 94.7°C, sensitivity parameters Δ_1 and Δ_2 of -15950 and -18830 and an equilibrium constant of 141.6. Transitions move together as salt concentration increases. This is shown in the temperature difference plot as the temperature difference between the two transitions.*
*Also shown on this figure are the results of optimal fitting to the same xanthan, but allowing for the residual ionic content of 4% (w/w) sodium in the dry sample. See **Table 1** for new parameter values and the text for further consideration of this point.*

When the effect of the other polysaccharides on the xanthan "charge" transitions is examined, the robustness of the peak temperatures to the presence of the other polysaccharides is seen (**Figure 5**). Only in a very few cases is there a suggestion of an effect, and these can qualitatively be explained by the changes in the charge on the polymer due to changes in the ratio of salt and polymer *i.e.* the effective equilibrium constant. This could be systematically investigated using the present model but this has not been done in the work reported here. Essentially the xanthans exhibit similar transition temperatures regardless of the presence of other polysaccharides with respect to the "charge" transitions. This may not be completely unexpected, as only charged polysaccharides might be expected to show a major effect in response to changes in salt concentration, however clearly other interactions such as hydrogen bonds and also interactions between backbones as mentioned briefly in the discussion are only having a minor effect and there is little synergy with regard to the basic charge based transitions. This is of course not the case for synergistic behaviour in the rheology of mixtures, for example of glucomannans and xanthan where large effects are seen and explained by interactions between the backbones of the molecules. An example of this can be seen on the lower trace of **Figure 5** where a large peak at approximately 60°C can be seen and is not directly related to transitions present in the components.

The small increases in transition temperature of the xanthans in the LPX+HPX mixture can be qualitatively assigned to effective increases in salt concentration perhaps because the HPX may come naturally with significant amounts of associated salt (Lad, Todd, Morris, MacNaughtan, Sworn, & Foster, 2013) although these effects at low concentrations of xanthan would be expected to be small. The changes in the SPX+LPX system are not easily explained. It is interesting however to speculate that there is perhaps an interchange of chains of differing pyruvate content of one species with the other, producing an averaging of transition temperatures. It is also interesting to note in a recent review by Morris (2019), that enthalpically stable coaxial dimerisation through non-covalent bonding between participating strands (helices), with interconversion between single-helix and double-helix structures is proposed, which may account for the slight differences seen here, now taken from an electrostatic explanation standpoint.

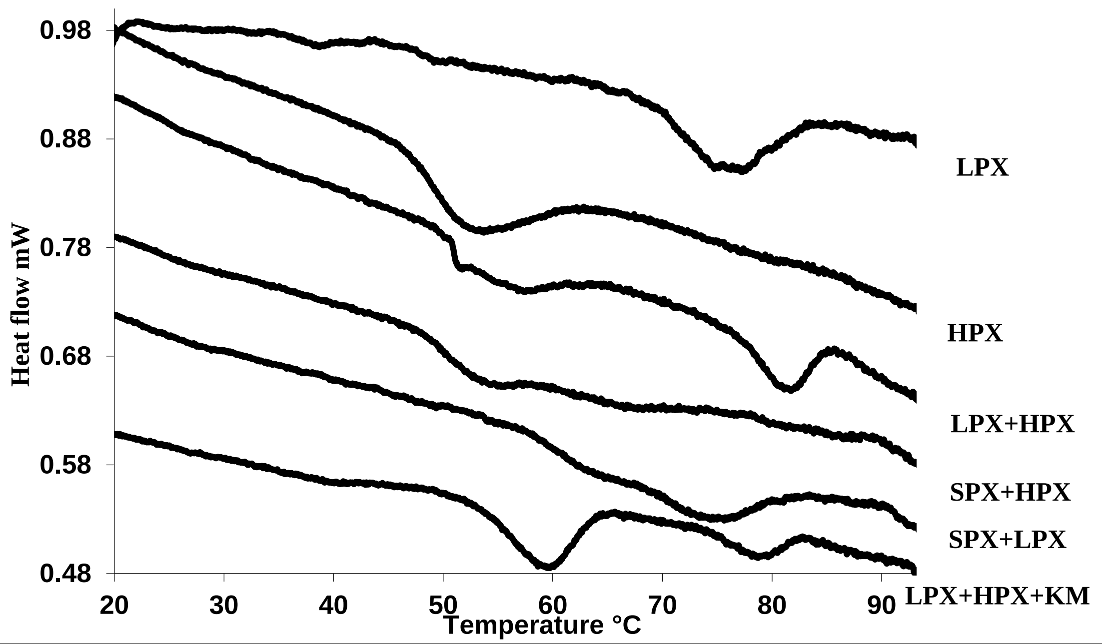

***Figure 5** shows selected transitions, concentrating on the interactions between xanthans. SPX standard pyruvate xanthan; LPX low pyruvate xanthan; HPX high pyruvate xanthan;*

KM konjac mannan. The distinct "backbone" interaction transition at 60 °C can be seen in the lower trace for the KM/xanthan mixture with an interaction between the KM and HPX appearing to take place leaving the LPX reduced in intensity but otherwise relatively unaffected. All samples were run at 10 mM concentration NaCl however the polymer mixtures are kept to an overall concentration of 1% (individual concentrations being 0.5% in mixtures) hence the concentration of individual polymers is lower in mixtures and the effective salt concentration higher accounting for the shifts to higher temperature in the case of the LPX+HPX mixture for example. This argument does not appear to hold for the SPX+LPX system implying a more complex interplay of factors.

Using a selection of data for HPX and LPX, transition temperatures have been plotted on **Figure 6** together with the data shown on **Figure 4.** Sub-optimal theoretical plots for the individual HPX and LPX samples have been obtained by optimising on the SPX transitions but setting the limiting transition temperature arbitrarily to 120°C. The plots for the HPX and LPX are constructed using the fitting parameters derived for the high and low pyruvate phases observed in the SPX. The data for the low salt concentration and higher pyruvate xanthan do not fit well to the curves. This situation corresponds to an extreme charge situation and the simple model for charge effects fails in these situations. However, in "typical" situations the simple model seems to work reasonably well.

The fit is now sub-optimal for the SPX (see **Table 1**) and the poor fit for the HPX is thought to reflect the tendency of HPX to have a relatively large ionic content associated with the high negative charge density on the molecule. The HPX points should therefore be displaced to the right on the graph producing a better fit. The effect of temperature on the equilibrium constant has not been taken into account in this work. It has been pointed out to us that depending on the heat changes on the binding of sodium to pyruvate, the equilibrium constant will increase for an endothermic reaction and hence reduce the negatively charged species. This will have the effect of increasing transition temperatures. This could be part of the explanation for the dramatically increased values of transition temperature at high sodium contents. Tests for all these proposals are needed in future work and would require extensive and extremely accurate data.

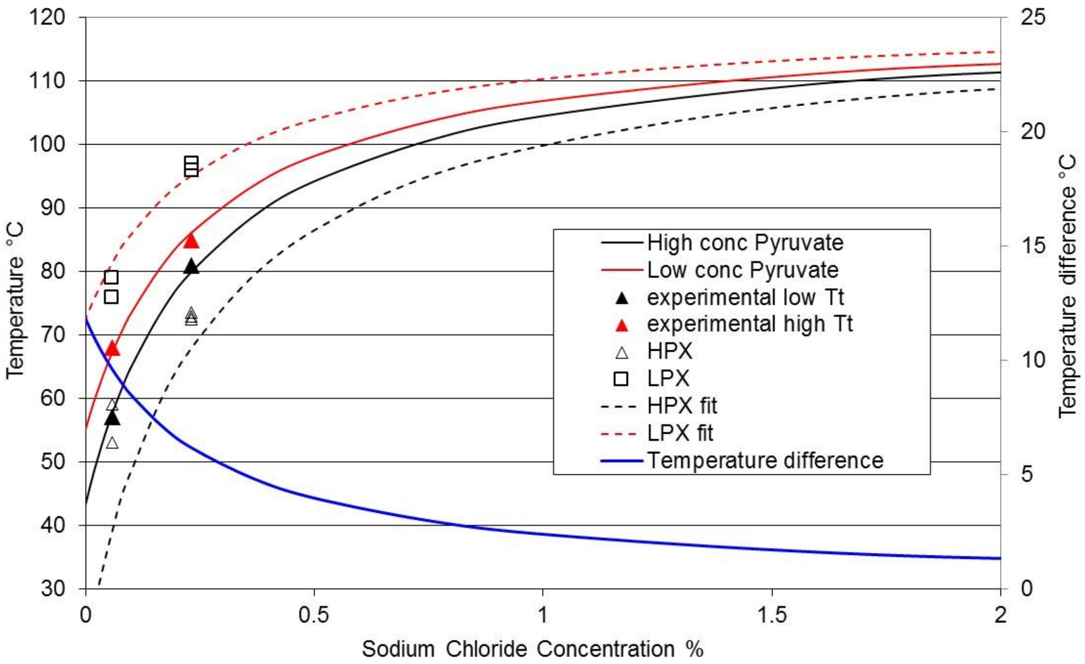

Figure 6 *shows the predicted transition temperatures for the 2 phases as a function of salt concentration with the maximum xanthan transition temperature arbitrarily set to 120°C. The data for the high (HPX) and low (LPX) pyruvate xanthan at a concentration of 1% are added to the plot. The additional HPX and LPX curves use the same equilibrium constant and Tm as for the standard plot, but use the sensitivity parameters for the high pyruvate and low pyruvate phases observed in the standard xanthan respectively, and hence are non-optimised. See* ***Table 1*** *for parameter values.*

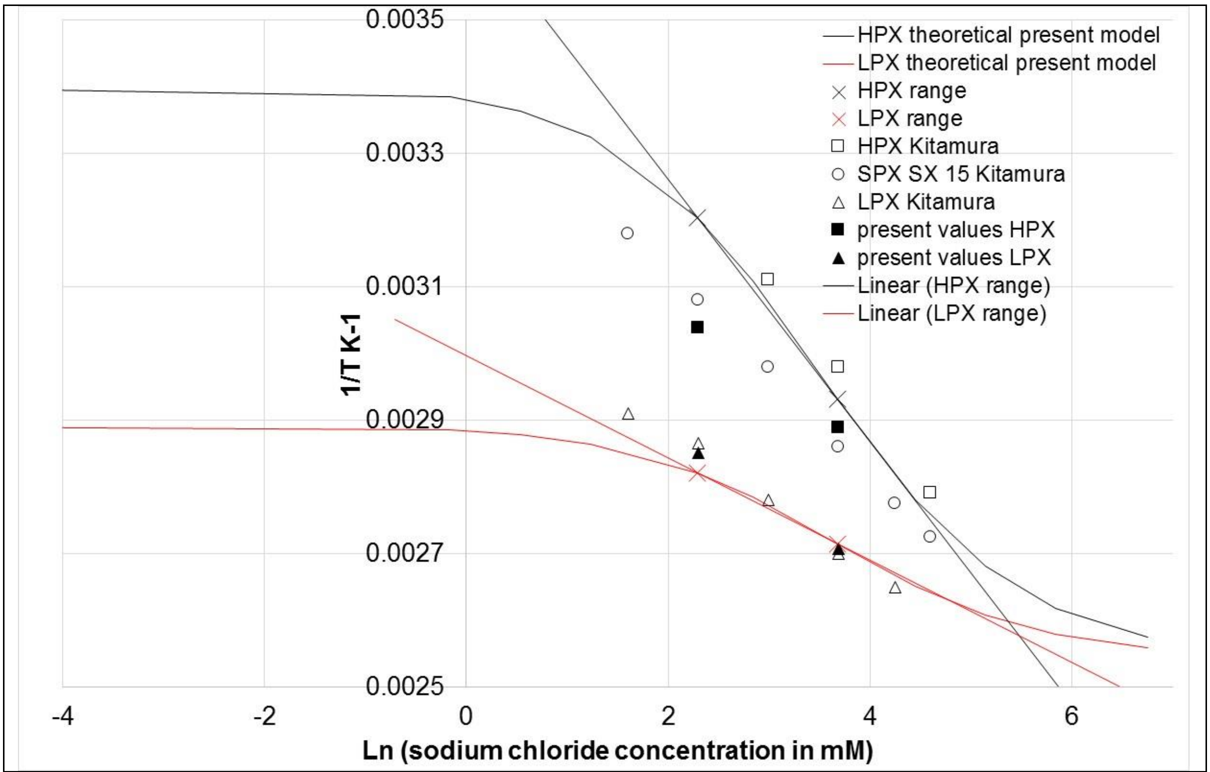

***Figure 7** shows a widely used plot of the natural logarithm of the sodium chloride concentration in mM against the reciprocal of the transition temperature in Kelvin. The lines are the theoretical plots over the range of salt concentration used in the present experiments. Data from the literature (*Kitamura, Takeo, Kuge, & Stokke, 1991*) are also shown on this plot.*

3.1 Residual salt content and chain mixing

Closer examination of **Figure 5** which mainly shows the interactions between the charged xanthans suggests that there are differences in transition temperature values and peak shapes upon interaction, and that the lack of effect of other charged polysaccharides reported in the above discussion may only be correct to a first approximation. If we consider the LPX+HPX system, both individual transitions appear to be increased in temperature and the lower (HPX) transition is broadened; perhaps even endowed with a biphasic nature. It has already been stated that the lower concentration of polymer and the consequent higher effective salt concentration could qualitatively explain these effects. However other factors may be at play. The explanation for the HPX broadening and raised temperature may lie in the mixing of chains of different pyruvate content, and subsequent interconversion between single and double helices, as outlined earlier and in Morris (2019). A mixture of LPX + HPX chains would be expected to have a higher transition temperature and a broader peak. Another explanation for the raised transition temperature of the LPX system may lie in the residual salt content. It was observed in these experiments that transition temperatures were very sensitive to salt content at the lower level (10 mM) and could have rather variable values. This is almost certainly due to residual levels of salt present in the original xanthan powders. We propose that the HPX xanthan will have higher levels of residual salt due to the higher inherent pyruvate content/charge of the molecule, which would then have an increased effect on the lower pyruvate system (increasing the transition temperature of the LPX xanthan) by a similar mechanism to our proposed simple mass action model.

Table 1** shows the % pyruvate contents for the xanthans and details of optimal and sub-optimal fit parameters. The pyruvate values for SPX are calculated as described in reference Abbaszadeh, et al. (2015) and the values in that reference are used here. Phase 1 is the high pyruvate low temperature phase. Calculations for the model were conducted on a molar basis using a molecular weight for the pyruvate of 88.* ** *= sub-optimal fit. The "Fit quality" is the sum of the square of the differences between experimentally determined transition temperatures and the theoretical temperatures predicted by the model.*

Parameter	**SPX (1K 2 Δ values) optimal**		**SPX (1K 2 Δ values) optimal (added ions)**		**SPX (1K 2 Δ values) Tm set to 120°C**		**LPX***	**HPX***
% Pyruvate	**3**	**5**	**3**	**5**	**3**	**5**	**2.2**	**6.5**
K (Litres/Mole)	141.6		270		23.1		23.1*****	23.1*****
Sensitivity $\Delta_{1\ HP}$ (°C Litres/Mole)	-	-15950	-	-68800	-	-13500	-	-13500*****
Sensitivity $\Delta_{2\ LP}$ (°C Litres/Mole)	-18830	-	-89400	-	-19000	-	-19000*****	-
T_m °C	94.7		104.3		120*****		120*****	120*****
Fit quality	$<10^{-5}$		0.25		0.83		-	-

3.2 The contrast of the effect of pyruvate and glucuronic acid

Figure 7 shows a plot of the natural logarithm of the sodium concentration vs. the reciprocal of the absolute value of the transition temperature in Kelvin. Linearity of this type of plot is purported to be evidence of the applicability of the Manning theory for charged polyelectrolytes and has been reported in many publications. It can be seen that over the concentration region of salt used in the present experiments and using the present simple model, the plot is also essentially linear. Similarly, data taken from the literature (Kitamura, Takeo, Kuge, & Stokke 1991) show that the present model would be linear over the salt concentration range of most reported experiments. Strictly speaking, the Manning theory (Manning 1970) is not applicable to polyelectrolytes in this relatively high concentration region (1% = 10mg/ml) and is also formulated on a linear array of point charges, not charges distributed around a helix. The linearity does not appear to be a particularly demanding test of the applicability of the Manning theory. Other tests have been proposed such as counterion condensation (Bordi, Cametti, & Paradossi, 1996) from electrical conductivity measurements.

It is interesting to speculate why such a simple proposal actually appears to account for the major observations here when the glucuronate with similar properties to the pyruvate should be present in higher concentrations on the xanthan chain. Steric models of xanthan show the glucuronate tucked away close to the backbone whereas the pyruvates are located at the outside of the helical structure (Smith, Symes, Lawson, & Morris, 1981, Brunchi, Bercea, Morariu, & Avadanei, 2016, Morris, 2019) and hence has greater flexibility. It is believed that this key location and the ability to interact more easily are key to the pyruvate controlling the charge interactions.

This is apparently contradicted by the observation that in the absence of the terminal mannose and consequently pyruvate there is still an increase in transition temperature with increasing salt content (Christensen, Knudsen, Smidsrød, Kitamura, & Takeo, 1993). **Table 2** shows the values in the present work for the slope of the logarithm of the change in concentration divided by the change in reciprocal absolute transition temperature, compared with literature values. However, the different values for the slope between the HPX and LPX systems demonstrate that the glucuronic acid, despite being present in higher concentrations, does not account for the behaviour at different charge densities. Interestingly the slope increases for a decrease in the overall potential charge on the polymer as measured by both the slightly lower glucuronic acid content for the treated sample from the literature and the LPX polymer in the present work. As the salt might be expected to act similarly on both the glucuronic acid and the pyruvate groups, both having similar pKa values, the effect of the pyruvate can be viewed as superimposed upon but acting independently of the effect of glucuronic acid and the glucuronic acid effect becoming dominant when the pyruvate is removed.

Table 2 *shows data for the slope of the logarithm (and natural logarithm) of the change in concentration divided by the change in reciprocal absolute transition temperature from the literature (Christensen, et al 1993) compared with values from the present work. Also shown are the results for the removal of the terminal mannose and slight reduction in glucuronic acid content. Note that the slopes here are the reciprocals of the usual plots of this type of data (for example in* ***Figure 7****) in order to facilitate comparison with the values found in (Christensen, et al 1993).*

Parameter	Literature values for terminal mannose removed xanthan		Present values	
d log(conc M)/d (1/T^{-1})	3415	3002	-2204	-5664
d ln(conc mM)/d (1/T^{-1})	7863	6912	-5075	-13042
fβMannose	0.06	1	1	1
fGlcA	0.96	1	1	1
Pyruvate content	0	0	6.5	2.2

3.3 Residual ionic content

Despite the xanthans here having been dialysed against water, it is possible that a significant ionic content remains in the freeze dried xanthans. A cursory glance through the literature reveals that whilst most cited literature reports dialysis against water or salt solutions, some published work is unclear or unspecified. It was decided to use the manufacturer's measured value for sodium content of ~4% for a typical dry xanthan (see **Table 1** in Lad et al. (2013) for more details), convert this into a sodium chloride equivalent and to fit the data again. This ionic concentration is a typical value for a dry xanthan; the values for xanthans containing different levels of charged groups may well be different. The results of the fitting are shown on **Figure 4** and **Table 1**. In the model, the change in ionic concentration of the solution changes the charge on the xanthan and so changes the fitting parameters substantially, however the basic message of the model, namely that the 2 transitions approach each other in temperature as the concentration is increased, remains. These adjustments for the residual ionic content of the xanthan are important in that the changes in concentration of the solution are potentially substantial for incompletely dialysed material, particularly at low concentrations of added salt. This conclusion applies of course, to all reported work of this type.

4. Conclusions

An explanation for the differential effect of salt on the biphasic transitions observed in SPX has been given which appears to also hold when residual ions associated with the xanthan are taken into account. To a first approximation the effects of other polysaccharides on the thermal "charge" transitions due to xanthan were small. Interactions between different xanthans are however detectable. Explanations for all these effects are given in terms of charge interactions of salt with the polymers together with the possibility of chain mixing. There is a linear relation between the natural logarithm of the salt concentration and the reciprocal of the transition temperature in Kelvin. This simple model may be of use in the interpretation of the effects of electrolytes on other charged systems and may have an impact on whether xanthan is in a single or double helix conformation.

5. Acknowledgements

Part of the research leading to these results (AA) was funded by the European Community's Seventh Framework Program (FP7/2007-2013) under Grant Agreement No. 214015. We would like to thank Dr. Graham Sworn, Mr. Emanuel Kerdavid and Mr. José Fayos of the DuPont, Danisco Company for partially funding (ML, GAM and WM), and for preparing, characterizing and providing the xanthan samples.

6. References

Abbaszadeh, A., MacNaughtan, W., Sworn, G., & Foster, T. J. (2016). New insights into xanthan synergistic interactions with konjac glucomannan: A novel interaction mechanism proposal. *Carbohydrate Polymers*, **144**, 168-177.

Abbaszadeh, A., Lad, M., Janin, M., Morris, G. A., MacNaughtan, W., Sworn, G., & Foster, T. J. (2015). A novel approach to the determination of the pyruvate and acetate distribution in xanthan. *Food Hydrocolloids*, **44**, 162-171.

Agoub, A. A., Smith, A. M., Giannouli, P., Richardson, R. K., & Morris, E. R. (2007). "Melt-in-the-mouth" gels from mixtures of xanthan and konjac glucomannan under acidic conditions: A rheological and calorimetric study of the mechanism of synergistic gelation. *Carbohydrate Polymers*, **69**, 713-724.

Annable, P., Fitton, M. G., Harris, B., Phillips, G. O., & Williams, P. A. (1994). Phase behaviour and rheology of mixed polymer systems containing starch. *Food Hydrocolloids*, **8**, 351–359.

Bordi, F., Cametti, C., & Paradossi, G. (1996). Conformational changes of xanthan in salt-free aqueous solutions: a low-frequency electrical conductivity study. *The Journal of Physical Chemistry*, **100**, 7148-7154.

Bresolin, T. M.B., Milas, M., Rinaudo, M., Reicher, F., & Ganter, J. L. M. S. (1999). Role of galactomannan composition on the binary gel formation with xanthan. *International Journal of Biological Macromolecules*, **26**, 225-231.

Brunchi, C-E., Bercea, M., Morariu, S., & Avadanei, M. (2016). Investigations on the interactions between xanthan gum and poly(vinyl alcohol) in solid state and aqueous solutions. *European Polymer Journal*, **84**, 161-172.

Burchard, W. (2001). Structure formation by polysaccharides in concentrated solution. *Biomacromolecules*, **2**, 342-353.

Christensen, B. E., Knudsen, K. D., Smidsrød, O., Kitamura, S., & Takeo, K. (1993). Temperature-Induced conformational transition in xanthans with partially hydrolyzed side chains. *Biopolymers*, **33**, 151-161.

Christensen, B. E., & Smidsrød, O. (1991). Hydrolysis of xanthan in dilute acid: Effects on chemical composition, conformation, and intrinsic viscosity. *Carbohydrate Research*, **214**, 55-69.

Goycoolea, F. M., Morris, E. R., & Gidley, M. J. (1995). Screening for synergistic interactions in dilute polysaccharide solutions. *Carbohydrate Polymers*, **28**, 351-358.

Khouryieh, H.A., Herald, T.J., Aramouni, F. & Alavi, S. (2007). Intrinsic viscosity and viscoelastic properties of xanthan/guar mixtures in dilute solutions: Effect of salt concentration on the polymer interactions. *Food Research International*, **40**, 883-893.

Kitamura, S., Takeo, K., Kuge, T., & Stokke, B. T. (1991). Thermally induced conformational transition of double-stranded xanthan in aqueous salt solutions. *Biopolymers*, **31**, 1243-1255.

Kool, M. M., Schols, H. A., Delahaije, R. J. B. M., Sworn, G., Wierenga, P. A., & Gruppen, H. (2013). The influence of the primary and secondary xanthan structure on the enzymatic hydrolysis of the xanthan backbone. *Carbohydrate Polymers*, **97**, 368-375.

Lad, M., Todd, T., Morris, G. A., MacNaughtan, W., Sworn, G. & Foster, T. J. (2013). On the origin of sharp peaks in the x-ray diffraction patterns of xanthan powders. *Food Chemistry*, **139**, 1146-1151.

Manning, G. S. (1970). On the interpretation of conductance measurements in salt-free polyelectrolyte solutions with an application to the helix–coil transition of poly (D-glutamic acid). *Biopolymers*, **9**, 1543-1546.

Morris, E. R. (1990). Mixed polymer gels. In P. Harris (Ed.), Food gels (pp. 291–360). Elsevier Applied Science: London, UK, pp. 291-359.

Morris, E. R. (2019). Ordered conformation of xanthan in solutions and "weak gels": Single helix, double helix – or both? *Food Hydrocolloids*, **86**, 18-25.

Morris, E. R., Rees, D. A., Young, G., Walkinshaw, M.D, & Darke, A. (1977). Order-disorder transition for a bacterial polysaccharide in solution. A role for polysaccharide conformation in recognition between *Xanthomonas* pathogen and its plant host. *Journal of Molecular Biology*, **110**, 1-16.

Morris, G. A., & Harding, S. E. (2009). Polysaccharides, Microbial. In: Schaechter, M., Ed. Encyclopedia of Microbiology (Third Edition). Elsevier: Amsterdam, Netherlands, pp. 482-494.

Morris, G. A., Puaud, M., Li, P., Lui, Z., Mitchell, J. R. & Harding, S. E. (2001). Hydrodynamic characterisation of the exopolysaccharide from the halophilic cyanobacteria *Aphanothece halophytica* GR02: a comparison with xanthan. *Carbohydrate Polymers*, **44**, 261-268.

Morris, V. J., & Wilde, P. J. (1997). Interactions of food biopolymers. *Current Opinion in Colloid & Interface Science*, **2**, 567-572.

Morrison, N.A., Clark, R. Talashek, T. & Yuan, C. R. (2004). New forms of xanthan gum with enhanced properties. In *Gums and Stabilisers for the Food Industry 12*, eds. P. A. Williams and G. O. Phillips, Royal Society of Chemistry: Cambridge, UK, pp. 124-130.

Pastor, M. V., Costell, E., Izquierdo, L., & Durán, L. (1994). Effects of concentration, pH and salt content on flow characteristics of xanthan gum solutions. *Food Hydrocolloids*, **8**, 265-275.

Shatwell, K. P. & Sutherland, I. W., Dea, I. C. M., & Ross-Murphy, S. B. (1990). The influence of acetyl and pyruvate substituents on the helix-coil transition behaviour of xanthan, *Carbohydrate Research*, **206**, 87-103.

Smith, I. H., Symes, K. C., Lawson, C. J., & Morris, E. R. (1981). Influence of the pyruvate content of xanthan on macromolecular association in solution. *International Journal of Biological Macromolecules*, **3**, 129-134.

Verwey, E. J. W., & Overbeek, J. T. G. (1955). Theory of the stability of lyophobic colloids. *Journal of Colloid Science*, **10**, 224-225.

Williams, P. A., & Phillips, G. O. (1995). In *Food Polysaccharides and Their Applications*; Stephen, A. M., Ed.; Marcel Dekker: New York, pp. 463-500.